GEOELECTRICAL TECHNIQUES FOR SUBSURFACE CHARACTERIZATION AND CONTAMINANT PLUME IMAGES AT LANDFILL SITES

ABDULLAHI ABDULRAHMAN

UNIVERSITI SAINS MALAYSIA

2016

GEOELECTRICAL TECHNIQUES FOR SUBSURFACE CHARACTERIZATION AND CONTAMINANT PLUME IMAGES AT LANDFILL SITES

by

ABDULLAHI ABDULRAHMAN

Thesis submitted in fulfilment of the requirements
for the degree of
Doctor of Philosophy

August 2016

ACKNOWLEDGEMENT

First and foremost, I thank Almighty Allah for bestowing knowledge upon me and for giving me this great opportunity to pursue a doctoral degree. This work is dedicated to Prophet Muhammad (May the peace and blessings of Allah be upon him), being the source of my inspiration, then to my parents, late Alhaji Abdurrahman Hassan Enagi and Hajiya Hajara Idris Enagi, including my step mother, Hajiya Habiba Abdullahi Enagi, for the effort in my upbringing and the unflinching support of my educational pursuits.

I would like to express my deepest gratitude to Prof. Mohd Nawawi Bin Mohd Nordin, my mentor, for guiding me through this process with his experience and knowledge. I sincerely thank him for motivating me all the way during my doctoral journey and for allowing me to work at my pace. The constructive feedbacks I received from him strengthened the final product of my research. I thank my two co-supervisors, Associate Prof. Rosli Bin Saad, and Associate Prof. Asad Siraj Abu-Rizaiza for their unwavering support throughout the study period. The assistance of Associate Prof. Mohd Suffian Yusoff in arranging the access to the landfill sites is highly appreciated. My gratitude also to Associate Prof. Amin Esmail Khalil and Associate Prof. Hassan Mohamed Baioumy for their contributions to the review of publication manuscripts. I acknowledge Dr Nur Azwin Ismail and Dr Taiwo Abdul-Wahab Owolabi for guiding me through the statistical analyses portion of my research. I thank my colleagues, Dr Nordiana Mohd Muztaza, Dr Kola Abdul-Nafiu Adiat, Dr Saheed Kehinde Ishola, Mr John Stephen Kayode and Dr Bashir Kayode Sodipo for the valuable suggestions throughout this process. My appreciation also to Dr Nasir

Khalid Abdullahi of Kaduna State University for a timely aid during data acquisition in Nigeria.

The field support from Messrs Mydin Bin Jamal, Low Weng Leng, Yaakub Bin Othman, Shahil Ahmad Khosaini, and the humorous Azmi Bin Abdullah, is paramount to the success of the research. I humbly appreciate the continued cooperation from these technical staff. My appreciation also to the School of Civil Engineering, USM for the use of its laboratories and the support from the technical staff, Messrs Mohad Shukri Zambri, and Mohammed Nizam Mohd Kamal. I thank Mr Hossein Farraji and Dr Kehinde Fagbenro for the support in conducting the physicochemical analyses. My gratitude to Idaman Bersih Sdn Bhd and Majlis Daerah Kerian Bangai Serai for granting permission for use of the landfills selected for this study. My gratefulness also to the technical staff of Department of Physics, Abubakar Tafawa Balewa University Bauchi, Nigeria led by Mr Patrick G Aliyu, for their participation in the field work conducted at Bauchi, Nigeria.

Special thanks to Engineer Muhammad Bima Abdurrahman, Suleiman Abdurrahman, Aminu Abdurrahman, Yunusa Abdurrahman, Muhammad Hassan, Aisha Abdurrahman, Murtala Abdulrahman, Hassana Abdurrahman and other brothers and sisters who are excellent sources of inspiration. I thank my wives and life partners, beloved Fatima Umar Zambuk and Amina Musa Salihu, whose patience, understanding and support while with me in Malaysia and during my absence in Nigeria, allowed me to accomplish my mission. I am deeply indebted and forever grateful. My precious girls and boys, Khadija, Umar Farouq, Idris, Hassan, Muhammad Bashir, Aisha, and Abdurrahman, I do apologise for the many months that I was supposed to spend with them and thus missing some vital transition in their

upbringing. The encouragement from my fiancée, Aisha Muhammad Idris is also worth mentioning.

To my friends, Prof. Muhammad Ahmad AbdulAzeez, Dr Muhammad Abdulkarim, Mr Abdullahi Suleiman, Prof. Auwal Musa Tijjani, Mr Dauda Bakum Adamu, Mr Samuel Ben Mbang, Mr Ahmad Danladi Shehu, Engineer Isa Muhammad Doko, Engineer Abdulrahman Muhammad Lapai, Dr Muhammad Muhammad Ndamitso, Messrs Majin Adamu Santali, Abdullahi Muhammad Santa, Danladi Zayum, and My uncle and colleague, Engineer Ibrahim Idris Enagi, cousins, late Adamu Muhammad, Muhammad Bello Haruna, Muhammad Bashir and nephew, Ndabenu the Majidadi of Enagi. I am grateful for their confidence in me and to whom I enjoy the pleasure of working and association.

I would like to thank the Federal Government of Nigeria (FGN) and Abubakar Tafawa Balewa University (ATBU), Bauchi for finding me worthy to benefit from the Tertiary Education Trust Fund (TETFUND) academic staff development programme. Finally, I wish to convey my profound appreciation to the Academic Staff Union of Universities (ASUU) of Nigeria, being the brainchild of TETFUND, and most importantly for its continued struggle to uplift the standard of education in Nigeria.

TABLE OF CONTENTS

ACKNOWLEDGEMENT ..... **II**

LIST OF TABLES ..... **IX**

LIST OF FIGURES ..... **XII**

LIST OF ABBREVIATIONS ..... **XX**

LIST OF SYMBOLS ..... **XXII**

LIST OF APPENDICES ..... **XXIV**

ABSTRAK ..... **XXV**

ABSTRACT ..... **XXVII**

CHAPTER 1 − INTRODUCTION **1**

1.1 Background 1

1.2 Problem statements 5

1.3 Research objectives 8

1.4 Scope and limitations of the study 9

1.5 Thesis outline 10

CHAPTER 2 − LITERATURE REVIEW **11**

2.1 Introduction 11

2.2 Review of geophysical techniques 11

2.3 Previous geophysical studies on landfills 13
2.4 Joint resistivity/Induced Polarization (IP) surveys at landfill sites 21
2.5 Landfills in Malaysia 23
2.6 Landfill leachate 30
2.7 Electrical resistivity method 33
2.7.1 Basic principles 33
2.7.2 Instrumentation and data acquisition 42
2.7.3 Electrode array configurations 45
2.7.3(a) Wenner array 45
2.7.3(b) Dipole−Dipole array 47
2.7.3(c) Wenner−Schlumberger array 47
2.7.3(d) Pole−Pole array 48
2.7.3(e) Pole−Dipole array 48
2.7.4 Modelling 49
2.7.4(a) Forward modelling 49
2.7.4(b) Inverse modelling 52
2.7.4(c) Model misfit 54
2.7.5 Inversion algorithm 54
2.7.6 3D electrical resistivity surveys 56
2.8 Induced Polarization method 60
2.8.1 Basic principles of Induced Polarization 60
2.8.2 Induced Polarization measurements 62
2.8.3 Induced Polarization instrumentation and data acquisition 72
2.8.4 Modelling of Induced Polarization 73
2.8.5 Interpretation of Induced Polarization 75
2.9 Summary 77

CHAPTER 3 − METHODOLOGY 78

3.1 Introduction 78

3.2 Description of the study sites 79
3.2.1 Location and structure of study areas 79
3.2.2 General geology of Malaysia 94
3.2.3 Geology of the study sites 98
3.2.4 Climate of the study areas 98
3.3 2D resistivity/IP data acquisition and processing 99
3.3.1 2D resistivity/IP data acquisition 99
3.3.2 2D resistivity/IP data processing 108
3.4 Groundwater flow direction 112
3.5 Physicochemical analyses 115
3.6 2D resistivity/IP landfill characterization 121
3.7 3D resistivity/IP model for leachate mapping 122
3.8 Geostatistical analysis 129
3.9 Summary 130

CHAPTER 4 − RESULTS AND DISCUSSION 133

4.1 Introduction 133
4.2 2D characterization of landfill sites 133
4.2.1 Leachate plume assessment 134
4.2.2 Closed Ampang Jajar Landfill (AJL) site 140
4.2.3 Active Pulau Burung Landfill (PBL) site 147
4.3 Contaminant plume mapping 152
4.3.1 Porosity evaluation 154
4.3.2 3D leachate quantification 162
4.4 Data and statistical analyses 182
4.4.1 Geophysical and geotechnical data analysis 182
4.4.1(a) Regression analyses for the contaminated zone 184
4.4.1(b) Regression Analyses for the Uncontaminated Zone 191

4.4.1(c) Comparative Data Analysis 197
4.4.2 Physiochemical Data Analysis 204
4.5 Summary 213

CHAPTER 5 − CONCLUSIONS AND RECOMMENDATIONS 214

5.1 Conclusions 214
5.2 Recommendations for further work 216

REFERENCES 218

APPENDICES 235

LIST OF PUBLICATIONS 264

LIST OF TABLES

		Page
Table 2.1	Classification of geophysical methods [after Kearey et al. (2002)]	12
Table 2.2	Applications of geophysical methods [after Kearey et al. (2002)]	13
Table 2.3	Summary of application of geophysical surveys at landfill sites	19
Table 2.4	Existing landfills sites in Malaysia [after JPSPN, Malaysia (2012)]	23
Table 2.5	Classification of landfills in Malaysia [modified from Fauziah and Agamuthu (2012)]	25
Table 2.6	Sanitary Landfills in Malaysia in 2010 [adapted from Fauziah and Agamuthu (2012)]	25
Table 2.7	Typical composition of landfill leachate [adapted from Christensen et al. (2001)]	31
Table 2.8	Electrical resistivity range for different formations [adapted form Guerin et al. (2004)]	36
Table 3.1	Typical porosity values for different soils [adapted from (Geotechdata.info, 2013)]	120
Table 3.2	Lithology Logs showing porosity of soil columns at outskirts of Bauchi, Nigeria	128
Table 3.3	Computation of leachate volume at Bauchi using the eight 3D horizontal slices	128
Table 3.4	Inverse distance estimation for porosity using weighted average of the neighbouring sampled data	131
Table 4.1	Analyses of physicochemical parameters from leachate aeration ponds, surface/ground water samples at BL site	137
Table 4.2	The temperature and depth at sampling, phreatic levels, and lithology sections at BL	138
Table 4.3	Analyses of heavy metals from leachate and surface/ground water samples at BL site (All quantities are in mg/L)	139

Table 4.4	Adopted interpretation scheme of the resistivity and chargeability inverse models for the selected landfill sites	141
Table 4.5	Dimensions for determining groundwater flow at BL	152
Table 4.6	Borehole lithology logs indicating porosity of soils sampled at BL	155
Table 4.7	Porosity estimate for Unit H, Layer 1 at BL	158
Table 4.8	Porosity estimate for Unit C, Layer 1 at BL	158
Table 4.9	Porosity estimate for Unit G, Layer 1 at BL	159
Table 4.10	Porosity estimate for Unit A, Layer 1 at BL	159
Table 4.11	Porosity estimate for Unit E, Layer 1 at BL	160
Table 4.12	Porosity framework showing laboratory inferred and estimated values for the 12 layers at BL	161
Table 4.13	The magnitude of contaminated blocks for the eight porosity units in each of the 12 layers at BL	174
Table 4.14	Leachate estimate for Layer 1	174
Table 4.15	Leachate estimate for Layer 2	175
Table 4.16	Leachate estimate for Layer 3	175
Table 4.17	Leachate estimate for Layer 4	176
Table 4.18	Leachate estimate for Layer 5	176
Table 4.19	Leachate estimate for Layer 6	177
Table 4.20	Leachate estimate for Layer 7	177
Table 4.21	Leachate estimate for Layer 8	178
Table 4.22	Leachate estimate for Layer 9	178
Table 4.23	Leachate estimate for Layer 10	179
Table 4.24	Leachate estimate for Layer 11	179
Table 4.25	Leachate estimate for Layer 12	180

Table 4.26	Computation of leachate volume for the 12 layers	180
Table 4.27	Parameters at BH 1 representing contaminated zone	185
Table 4.28	Parameters at BH 2 representing uncontaminated zone	191
Table 4.29	The correlation between observed and calculated porosity values at the contaminated zone	201
Table 4.30	The correlation between observed and calculated porosity values at the uncontaminated zone	202
Table 4.31	The comparison of porosity estimates between the geostatistical approach and the use of empirical formulae	203
Table 4.32	Statistical treatment for analytical measurements of physicochemical pollution parameters for samples from aeration ponds, surface flows, and boreholes	205
Table 4.33	Pearson's statistical analysis of samples from aeration ponds, surface flows, and boreholes (linear correlation observed between the physiochemical parameters)	208
Table 4.34	Statistical treatment for analytical measurements of heavy metals for samples from aeration ponds, surface flows, and boreholes	209
Table 4.35	Pearson's statistical analysis of samples from aeration ponds, surface flows, and boreholes (linear correlation observed between the heavy metals)	212

LIST OF FIGURES

		Page
Figure 2.1	Decision-making process leading to the selection of geophysical methods and utility software for an investigation [adapted from (Reynolds, 1991)]	20
Figure 2.2	Open dumpsites in Malaysia	24
Figure 2.2 (a)	Active site in Kuala Terengganu	24
Figure 2.2(b)	Closed site at Parit Buntar, Perak	24
Figure 2.3	Bukit Tagar Sanitary Landfill Site [adapted from KUB-Berjaya Enviro Sdn Bhd, 2010 (www.kbenviro.com.my)]	26
Figure 2.3(a)	The polyethylene liner on waste	26
Figure 2.3 (b)	The leachate treatment system	26
Figure 2.4	Schematic illustrations of anaerobic and semi-aerobic landfills [adapted from (Aziz et al., 2010)]	28
Figure 2.5	Composition of household waste in Malaysia [after JPSPN, Malaysia (2012)]	29
Figure 2.6	Typical resistivity values of some soils, rocks, and minerals [after Loke (2015)]	35
Figure 2.7	Equipotential surfaces due to a current source [adapted from Loke (2015)]	37
Figure 2.8	Field configuration with two current (I) electrodes (C1 and C2) and two potential (V) electrodes (P1 and P2) [modified after Loke (2015)]	40
Figure 2.9	Sequence of measurements to build up a 2D pseudo section using the Wenner array (Loke, 2015)	43
Figure 2.10	ABEM Lund Imaging System, showing the multi-electrode application and added illustration for the roll-along technique (Dahlin, 1996)	43
Figure 2.11	Components of ABEM Lund Imaging System; TERAMETER SAS4000, ES10-64 ELECTRODE	44

	SELECTOR, 100 m cable rolls, cable-electrode connectors, steel electrodes and external 12 V DC supply	
Figure 2.12	Schematic representations of the survey arrays [after Loke (2015)]	46
Figure 2.13	Definition of electrical forward and inverse problem [modified after (Binley and Kemna, 2005)]	50
Figure 2.14	An arrangement of electrodes for 3D survey [after Loke (2015)]	57
Figure 2.15	The models used in the 3D inversion. (a) A standard model where the widths of the rectangular cells are equal to the unit electrode spacing in the x- and y-directions. (b) A model where the cells are divided in the horizontal direction [after Loke (2015)]	59
Figure 2.16	The overvoltage effect produced by IP after an applied current is switched off [after Reynolds (1997)]	61
Figure 2.17	Illustration of steps involved in membrane polarization [after Ward, (1990)]	63
Figure 2.18	Membrane polarization in rocks containing clay particles [after Ward, (1990)]	64
Figure 2.19	Illustration of the build up to electrode polarization [after Ward, (1990)]	65
Figure 2.20	Application of pulse current with alternate polarity and consequent measured voltage showing the effect of overvoltage Vp and rise-time on leading edge of the voltage pulse [after Reynolds, (1997)]	66
Figure 2.21	Two forms of measurement of overvoltage [after Reynolds, (1997)]	67
Figure 2.21(a)	At discrete time intervals $V(t_1)$, $V(t_2)$ and others	67
Figure 2.21(b)	By the area (*A*) beneath overvoltage curve	67
Figure 2.22	Range of chargeability values for some minerals, soils, and rock [after Loke, (2015)]	70
Figure 3.1	Map of Malaysia with neighbouring countries [adapted from (Wikipedia, 2015)]	79

Figure 3.2	Malaysia map in illustration with the provinces and the main cities and the inset indicates the locations of the landfills selected for this study [modified after (Dreamstime, 2015)]	80
Figure 3.3	Aerial view of AJL area showing landfill boundary, profiles A, B, C, D, E, F, and the control profile (CP)	82
Figure 3.4	Location map of AJL area showing profiles A, B, C, D, E, F, and the control profile	83
Figure 3.5	The solid waste compression system at the closed AJL site	84
Figure 3.6	Leachate Pond at AJL site	84
Figure 3.7	The closed AJL site with deposited garden waste	85
Figure 3.8	Aerial view of PBL site showing profiles G, H, J, K, L and the control line (CL)	86
Figure 3.9	Location map of PBL site showing landfill boundary, profiles G, H, J, K, L, and the control line	87
Figure 3.10	PBL site receiving both industrial and municipal solid wastes	88
Figure 3.11	The central leachate pond at PBL site	89
Figure 3.12	The gate of PBL site showing inlet and outlet waste measuring scales	89
Figure 3.13	The surveyed area at PBL with a gas ventilation pipe	90
Figure 3.14	Aerial view of BL area showing three of the eleven lines, L1, L6, and L10	91
Figure 3.15	Location map of BL area showing lines L1, L6, L10, and the borehole locations BH 1, BH 2, and BH 3	92
Figure 3.16	Deposited domestic waste at BL	93
Figure 3.17	The aeration ponds at BL showing the tipped leachate before its discharge to the nearby palm plantation	93
Figure 3.18	Non-operational waste measuring scale at BL	94
Figure 3.19	The Bauchi 3D inversion showing eight horizontal slices with corresponding depths where the values in the boxes on each side display the observed leachate areas.	95

Figure 3.20	Average and extreme monthly temperature pattern for Seberang Perai, Penang [adapted from (weather2, 2015)]	100
Figure 3.21	The average monthly distribution of rainfall for Seberang Perai, Penang indicating number of rainy days [adapted from (weather2, 2015)]	100
Figure 3.22	The direction of the gradient at AJL survey area based on the data acquisition profiles	101
Figure 3.23	The direction of the gradient at PBL survey area based on the data acquisition profiles	102
Figure 3.24	2D resistivity/IP data acquisition for the subsurface characterization at AJL site	103
Figure 3.25	2D resistivity/IP data acquisition for the subsurface characterization at PBL site	103
Figure 3.26	Three of the 11 survey lines downstream of BL indicating borehole positions	105
Figure 3.27	The photograph shows data acquisition on Line 1 crossing the leachate channel at the downstream of BL	106
Figure 3.28	Resistivity inverse model generated at a landfill site in Johannesburg, South Africa [adapted from Dahlin et al. (2010)]	110
Figure 3.29	Chargeability inverse model generated at a landfill site in Johannesburg, South Africa [adapted from Dahlin et al. (2010)]	111
Figure 3.30	The drilling equipment, photographs with the plantation owner and the combined team of drilling and geophysical data acquisition crew	113
Figure 3.31	Illustration of the water table elevation at three locations for determining groundwater floor direction (not drawn to scale)	114
Figure 3.32	Generating water table contours to determine direction of groundwater flow [adapted from Idaho Department of Environmental Quality, 2016 (www.imnh.isu.edu)]	114
Figure 3.33	The samples collection and in situ measurements at BL site	116

Figure 3.34	Varian 720/730-ES Inductively Coupled Plasma-Optical Emission Spectrometers used for analysis of heavy metals in samples from BL site	117
Figure 3.35	The heating and grinding of soil samples from BL site for porosity evaluation	118
Figure 3.36	3D electrical resistivity acquisition at the leachate quantification model site in Bauchi, Nigeria	125
Figure 3.37	2D resistivity inverse models at Bauchi, Nigeria (Profiles A, B, C, D, and E)	126
Figure 3.38	The Bauchi 3D inversion showing eight horizontal slices with corresponding depths where the values in the boxes on each side display the observed leachate areas	127
Figure 3.39	A flow chart illustrating summary of procedures in the methodology	132
Figure 4.1	Electrical resistivity and chargeability inverse models of the assessment Line 1 showing leachate units, IP anomalies, and borehole sections at BL	135
Figure 4.2	Electrical resistivity and chargeability inverse models of the assessment Line 6 showing leachate units, IP anomalies, and borehole sections at BL	135
Figure 4.3	Electrical resistivity and chargeability inverse models of the assessment Line 10 showing leachate units, IP anomalies, and borehole sections at BL.	136
Figure 4.4	Electrical resistivity and chargeability inverse models of profiles perpendicular to the slope of AJL depicting different strata beneath the landfill	142
Figure 4.4(a)	Profile A	142
Figure 4.4(b)	Profile B	142
Figure 4.4(c)	Profile C	142
Figure 4.5	Resistivity and chargeability models of profiles parallel to the slope of AJL distinguishing the strata beneath the landfill	143
Figure 4.5(a)	Profile D	143
Figure 4.5(b)	Profile E	143

Figure 4.5(c)	Profile F	143
Figure 4.6	Resistivity and chargeability inverse models of the control profile for AJL	146
Figure 4.7	Resistivity and chargeability inverse models of profiles perpendicular to the gradient of PBL, differentiating the landfill's subsurface	148
Figure 4.7(a)	Profile G	148
Figure 4.7(b)	Profile H	148
Figure 4.8	Resistivity and chargeability inverse models of profiles parallel to the gradient of PBL showing the classification of strata underneath the landfill	149
Figure 4.8(a)	Profile J	149
Figure 4.8(b)	Profile K	149
Figure 4.8(c)	Profile L	149
Figure 4.9	Resistivity and chargeability inverse models of the control profile for PBL	151
Figure 4.10	Groundwater flow direction determined by water table contours at the downstream of BL	153
Figure 4.11	Horizontal section of the survey area showing borehole points within delineated porosity units for the geostatistical computation	156
Figure 4.12	2D Resistivity and chargeability inverse models of Line 1 at BL	163
Figure 4.13	2D Resistivity and chargeability inverse models of Line 2 at BL	163
Figure 4.14	2D Resistivity and chargeability inverse models of Line 3 at BL	164
Figure 4.15	2D Resistivity and chargeability inverse models of Line 4 at BL	164
Figure 4.16	2D Resistivity and chargeability inverse models of Line 5 at BL	165

Figure 4.17	2D Resistivity and chargeability inverse models of Line 6 at BL	165
Figure 4.18	2D Resistivity and chargeability inverse models of Line 7 at BL	166
Figure 4.19	2D Resistivity and chargeability inverse models of Line 8 at BL	166
Figure 4.20	2D Resistivity and chargeability inverse models of Line 9 at BL	167
Figure 4.21	2D Resistivity and chargeability inverse models of Line 10 at BL	167
Figure 4.22	2D Resistivity and chargeability inverse models of Line 11 at BL	168
Figure 4.23	3D Resistivity and chargeability inverse models of Layers 1 and 2 at BL	168
Figure 4.24	3D Resistivity and chargeability inverse models of Layers 3 and 4 at BL	169
Figure 4.25	3D Resistivity and chargeability inverse models of Layers 5 and 6 at BL	169
Figure 4.26	3D Resistivity and chargeability inverse models of Layers 7 and 8 at BL	170
Figure 4.27	3D Resistivity and chargeability inverse models of Layers 9 and 10 at BL	170
Figure 4.28	3D Resistivity and chargeability inverse models of Layers 11 and 12 at BL	171
Figure 4.29	The 32 blocks of the horizontal section of Layer 1 for the computation of area of contamination (ΔA)	172
Figure 4.30	Variation of resistivity with depth at the contaminated location	185
Figure 4.31	Variation of chargeability with depth at the contaminated zone	186
Figure 4.32	Variation of porosity with depth at the contaminated zone	187
Figure 4.33	Variation of N value with depth at the contaminated zone	187

Figure 4.34	Relationship between chargeability and porosity at the contaminated zone	189
Figure 4.35	Relationship between chargeability and N value at the contaminated zone	189
Figure 4.36	Relationship between chargeability and resistivity at the contaminated zone	190
Figure 4.37	Variation of resistivity with depth at the uncontaminated zone	192
Figure 4.38	Variation of chargeability with depth at the uncontaminated zone	192
Figure 4.39	Variation of porosity with depth at the uncontaminated zone	193
Figure 4.40	Variation of N value with depth at the uncontaminated zone	194
Figure 4.41	Relationship between chargeability and porosity at the uncontaminated zone	195
Figure 4.42	Relationship between chargeability and N value at the uncontaminated zone	195
Figure 4.43	Relationship between chargeability and resistivity at the uncontaminated zone	196

LIST OF ABBREVIATIONS

ANOVA	Analysis of variance
APHA	American public health association
BOD	Biological oxygen demand
CMP	Common mid-point
COD	Chemical oxygen demand
DC	Direct current
DCPT	Dynamic cone penetration test
DMRT	Duncan’s multiple range test
EC	Electrical conductivity
EM	Electromagnetic
EPA	Environmental protection agency
FD	Finite difference
FE	Finite element
GPR	Ground penetrating radar
HDPE	High-density polyethylene
HELP	Hydrologic evaluation of landfill performance
IP	Induced polarization
MALM	Mise-à-la-masse
MASW	Multichannel analysis of surface waves
MF	Metal factor
MSW	Municipal solid waste
NAPL	Nonaqueous phase liquid
PFE	Percentage frequency effect

RMS	Root-mean-square
ROM	Read only memory
SAS	Signal averaging system
SBR	Sequential batch reactors
SP	Self-Potential
SPSS	Statistical package for social science
SPT	Standard penetrating test
TDS	Total dissolved solids
TOC	Total organic content
TSS	Total suspended solids
USA	United States of America
UXO	Unexploded ordinance
VLF	Very low frequency
WBM	Water balance method
WHO	World health organization

LIST OF SYMBOLS

'	Minute
"	Second
A	Ampere
E	Electric field intensity
ha	Hectare
Hz	Hertz
I	Electric current
I	Identity matrix
J	Electric current density
k	Boltzmann constant
K	Kelvin
m	Metre
M	Chargeability
n	Data level
N	N value
^{o}	Degree
^{o}C	Degree celsius
q_k	Model parameter change vector
r	Radius
R^2	Regression
S	Siemens
s	Seconds

Δ	Differential operator
δ	Dirac delta function
ε	Emissivity
λ	Damping factor
ρ	Electrical resistivity
σ	Electrical conductivity
Ω	Ohm
$\boldsymbol{\phi}$	Porosity
∇	Gradient

LIST OF APPENDICES

APPENDIX A BOREHOLE LITHOLOGY LOG DATA AT BERIAH LANDFILL SITE, ALOR PONGSU, PERAK

APPENDIX B REGULATIONS GOVERNING ACCEPTABLE CONDITIONS FOR DISCHARGE OF LEACHATE IN MALAYSIA

APPENDIX C INVERSION PARAMETERS AND SUMMARY OF RESULTS FROM 2D RESISTIVITY/IP MODELS GENERATED AT AMPANG JAJAR AND PULAU BURUNG LANDFILL SITES

APPENDIX D POROSITY ESTIMATES FOR THE EIGHT UNITS IN LAYERS 2 – 10 AT BERIAH LANDFILL SITE

APPENDIX E HORIZONTAL SECTIONS OF LAYERS 2 – 12 SHOWING THE 32 BLOCKS USED IN THE COMPUTATION OF AREA OF CONTAMINATION (ΔA) AT BERIAH LANDFILL SITE

APPENDIX F DETAILS OF STATISTICAL ANALYSES FOR PHYSICOCHEMICAL PARAMETERS INCLUDING THE HEAVY METALS SAMPLED AT BERIAH LANDFILL SITE

TEKNIK GEOELEKTRIK BAGI PENCIRIAN SUBPERMUKAAN DAN PEMETAAN KEPULAN BAHAN CEMAR DI TAPAK PELUPUSAN

ABSTRAK

Garis panduan tafsiran untuk analisis model songsangan yang dihasilkan bagi keberintangan elektrik dan kebolehcas di dua tapak pelupusan semi-aerobik yang dinaik taraf telah dibangunkan. Model songsangan yang dihasilkan daripada program songsangan 2D (RES2DINV) telah digunakan untuk menetapkan grid-grid pengimejan keberintangan dan kebolehcas di tapak pelupusan. Kajian mengesahkan bahawa keberintangan rendah (<10 Ωm) menunjukkan kepulan air larut lesap manakala unit kebolehcas tinggi (>70 ms) mewakili deposit sisa dan lapisan tanah liat tepu. Tambahan pula, sambutan IP pada kepulan air larut lesap hiliran yang disebarkan daripada tapak pelupusan separa aerobik yang berasingan telah dinilai. Penilaian juga meneliti status bahan cemar dan mengklasifikasikan strata di bawah tapak pelupusan perbandaran sisa pepejal. Hasil kajian menunjukkan kepulan yang didominasi oleh ion memaparkan zon kebolehcas yang lemah (<20 ms) dan menyokong polarisasi ionik berbanding polarisasi elektronik sebagai sambutan IP. Walau bagaimanapun, kepekatan ion yang tinggi dalam air larut lesap yang disebarkan menghalang polarisasi membran sekali gus mengurangkan kesan IP pada sedimen asal. Garis profil keberintangan dan kebolehcas dengan purata peratusan ralat mutlak lebih kurang 15% di tapak pencirian dan tapak penilaian menunjukkan zon berbeza pada strata subpermukaan. Perbandingan antara lajur air larut lesap di tapak pencirian mendedahkan bahawa tapak pelupusan tertutup dengan kadar deposit sisa yang lebih

tinggi mengandungi air larut lesap terkumpul yang lebih rendah berbanding tapak yang aktif. Model songsangan keberintangan 3D dan kebolehcas telah dihasilkan di tapak penilaian air larut lesap menggunakan program songsangan RES3DINV. Potongan mendatar daripada model songsang 3D telah digunakan untuk pemetaan bahan cemar dan pengkuantitian. Tambahan pula, analisis fisiokimia dan penilaian keliangan yang dijalankan di tapak ini masing-masing membolehkan penilaian kualitatif dan kuantitatif secara penuh dilakukan. Selain daripada takungan pengudaraan, keputusan fisiokimia mengesahkan bahawa beberapa indeks pencemaran yang diukur di kawasan hilir tapak kajian adalah tidak menepati kelulusan had pelepasan air larut lesap Malaysia. Anggaran keliangan bagi bahagian tanah tidak disampel menggunakan pendekatan geostatistik asas menyediakan platform untuk pengkuantitian air larut lesap di kawasan kajian yang berjumlah kira-kira 1.6×10^5 m^3 kepulan bahan cemar telah dianggarkan. Dalam proses ini, ungkapan empirik telah dihasilkan antara kuantiti geofizik dan geoteknik yang menggambarkan ciri-ciri hilir tapak pelupusan. Persempadanan tapak tercemar dalam kajian ini menyokong keberkesanan pemantauan kepulan bahan cemar dan boleh membawa kepada kaedah peninjauan yang menjanjikan bagi pemulihan atau penambakan tapak pelupusan sisa pepejal.

GEOELECTRICAL TECHNIQUES FOR SUBSURFACE CHARACTERIZATION AND CONTAMINANT PLUME IMAGES AT LANDFILL SITES

ABSTRACT

An interpretation template for the analysis of electrical resistivity and chargeability inverse models produced at two upgraded semi-aerobic landfill sites was developed. The inverse models generated from a 2D inversion program (RES2DINV) were used to set up grids of resistivity and chargeability imaging at the landfill sites. The study confirmed a low resistivity (<10 Ωm) depicting leachate plume while a high chargeability unit (>70 ms) represents waste deposits and saturated clayey layers. Furthermore, the IP responses of the disseminated leachate plume downstream of a separate landfill site were assessed. The appraisal also examines the contaminant status and classified the strata beneath municipal solid waste landfills. The outcome of the investigation showed that the ion-dominated plume displays a weak chargeability zone (<20 ms) and supports ionic polarization rather than electronic polarization in its IP responses. However, the high concentration of ions in the diffused leachate inhibits the membrane polarization, thus reducing the IP effects in host sediments. The outline of resistivity and chargeability profiles with average percentage error of about 15% at the characterization sites and assessment site shows differentiated zones of the subsurface strata. Comparison of the leachate columns at the characterization sites revealed that the closed landfill with a higher proportion of waste deposits contained a lesser accumulation of leachate than the active site. 3D resistivity and chargeability inverse

models were generated at the leachate assessment site using the RES3DINV inversion program. The horizontal slices from the 3D inverse models were utilized for the contaminant plume mapping and quantification. Additionally, physiochemical analysis and porosity evaluation conducted at this site enabled a full qualitative and quantitative assessment respectively. Despite the aeration ponding, the physiochemical results confirmed that some of the pollution indices measured at the downstream of the site were not within the Malaysian approved leachate discharge limits. The porosity estimation for the un-sampled soil sections using a basic geostatistical approach provided the platform for leachate quantification at the survey area where a total of about 1.6×10^5 m^3 amount of contaminant plume was estimated. In this process, empirical expressions were derived between geophysical and geotechnical quantities portraying the characteristics of downstream of a landfill site. Delineation of the contaminated sites in this study supports the effectiveness of contaminant plume monitoring and could lead to a promising reconnaissance tool for remediation or reclamation of solid waste disposal sites.

CHAPTER 1

INTRODUCTION

1.1 Background

The current best practices for sustainable solid waste management introduced a hierarchy of integrated resource management options that has been accepted worldwide; (i) prevention, (ii) reduction, (iii) recycling, (iv) disposal (Donevska et al., 2013). However, alternative waste management strategies such as incineration and composting have been developed to trim down the amount of waste for disposal. Waste minimization at the source is the cheapest and the most efficient waste management procedure. Minimization of the waste generation at the source and recycling are encouraged to improve the use of funds for disposal of solid waste. Though, even after application of a combination of these waste management methods, residuals are still left, which are usually deposited in a landfill. In landfilling, the waste decomposes under controlled conditions until its transformation into relatively inert and stabilized substance. This biodegradation involves the chemical and biochemical processes responsible for the decomposition of the waste materials (Kale et al., 2010) while the eventual result reduces the adverse environmental effects and other risks and inconveniences.

Despite the placement at the bottom of the hierarchy of options for integrated waste management, landfilling is the most commonly used disposal method for municipal and industrial solid wastes worldwide (Morris and Barlaz, 2011). The

existing trend in solid waste management is the sanitary landfilling which is widely employed in the developed world. However, the developing countries are still primarily engaged in open dumping and unregulated landfills (Singh et al., 2011). The potential of risk from the uncontrolled landfills and dumpsites exists in these countries. The resultant leachate produced due to waste transformation and rainfall can be identified by specific characteristics and variables, corresponding to high-strength wastewaters, which generate impacts and risks in the environment (Şchiopu et al., 2012).

In sanitary landfills, monitoring wells are usually installed within and around active and closed sanitary landfills to gauge the extent of contamination of groundwater (Pearce et al., 2011). Furthermore, the accumulated plume undergoes either biological and/or chemical treatment before discharge into natural aquifers. The application of sampling approach in monitoring landfills is invasive and may not intercept the contaminant plumes. Non-invasive, cost-effective and fast surface geophysical surveys are complementary tools to the monitoring wells to avoid intrusion into hazardous materials (Joshi, 2013). The geophysical methods are capable of discerning the distribution of leachate in landfills and its environs and suggest appropriate locations for the monitoring wells. The combination of geophysical investigation with a physiochemical analysis of leachate/groundwater samples from the monitoring wells determines the state of stabilization of the landfills (Vaudelet et al., 2011).

Among geophysical techniques, the electrical resistivity method is the most utilized in delineating solid waste disposal site. The electromagnetic method is oversensitive to metallic objects that are unfortunately very common at landfills, and

for this reason, the method is often discarded (Leroux et al., 2007). Magnetic methods distinguish waste boundaries because of its metallic content. On the other hand, the disseminated contaminant plume outside the landfill margins with minimal metallic substance would be poorly discerned using this approach. Several authors characterized landfill sites using electrical resistivity imaging (Rucker et al., 2010, Rucker et al., 2011, Li et al., 2012, Genelle et al., 2012, Abudeif, 2015, Sirieix et al., 2015). Additionally, in the case of bioreactor landfills, where leachate is recirculated to aid waste decomposition, the resistivity technique is employed to monitor the distribution of moisture within the landfill (Clement et al., 2010, Hossain et al., 2011, Clement et al., 2011).

The waste and leachate plume contain a high concentration of charges that lowers the resistivity of contaminated zones. However, methane gas at landfill sites generates high resistivity. These low and high resistivity values distinguish the areas from the surroundings and renders the resistivity approach an attractive tool for delineation of landfills. Electrical resistivity imaging is a relatively well-known method and has been used for some landfill applications (Rosquist et al., 2011). Though, in areas where the background is the moderate or low resistivity, typical landfill material may have similar resistivity to the background, and, therefore, indistinguishable from surroundings. Even in some higher resistivity settings, lower resistivity landfill material is easily confused with backfilled excavations, given the fact that many old landfills were quarry sites. Finding landfills near old, backfilled excavations is typical. Moreover, both a landfill and a backfilled excavation will show a negligible resistivity contrast with the background, and are therefore easily confused.

As a result of this minimal contrast, resistivity surveys (and also conductivity) often do not have sufficient data sets for waste site delineation (Carlson et al., 2001).

The incorporation of Induced Polarization (IP), which is a capacitive property of the subsurface, with electrical resistivity, assists in distinguishing between clay and sand bearing salt water both of which show low resistivity. Saline water that has high ionic conductivity depicts poor chargeability in contrast with clayey layers that generate strong IP response (Martinho and Almeida, 2006). Gazoty et al. (2012a) assert that ambiguities are produced in electrical resistivity surveys when the water table is within the waste layers. The dependence of the process on pore fluid introduces significant uncertainties in landfill mapping. The integration of electrical resistivity and IP removes some of the uncertainties and ambiguities embedded in the separate utilization of the techniques.

While the resistivity method responds to saturation, the IP is favoured towards the lithology and chargeable units associated with landfills (Legaz et al., 2010). Despite the challenges in instrumentation and data acquisition of IP surveys using conventional equipment, several case studies showed the desirability of combining the two methods to enhance characterization of landfills (Dahlin et al., 2010, Ustra et al., 2012, Gazoty et al., 2012a).

For a comprehensive appraisal of dumpsites, laboratory evaluation of the groundwater and soil samples, and the identification of geologic sections complements the geoelectrical results in the interpretation of the landfill's subsurface (Dahlin et al., 2010). Moreover, the physicochemical analyses determine the contrast in quality of plumes from the landfills to establish the degree of contamination. Paradis et al. (2014) emphasized the need for representative data that captures the spatial

distribution of groundwater flow and contaminant transport for aquifer management or remediation. A complete characterization of landfills delineates the buried materials, the soil sections, and the spread and intensity of contaminant leachate, staging the landfill for remediation, mining, or land reclamation.

1.2 Problem statements

In the application of electrical resistivity and IP techniques to delineate landfills' subsurface, the data acquisition and interpretation of electrical resistivity inverse models at the dumpsites is more definite than the analysis of chargeability inverse models. The weak signals from IP make its data acquisition with conventional resistivity meters and steel electrodes susceptible to noise and thus unreliable.

Sediment resistivity depends on the ratio of the gas and water volume in the pores, as well as on the temperature, the salinity of the pore fluid and the overall porosity (Rosquist et al., 2011). Low resistivity values are typical of seawater, brackish water, leachate, clay, solid waste, and fresh water. These values are due to the high concentration of ions and other charge carriers, thus increasing the conductivity of the subsurface. Intermediate resistivity values are associated with wet sand, sandstone, and limestone formations while high resistivity corresponds to dry sand or granite bedrock (Guérin et al., 2004).

There exists a high degree of certainty in distinguishing clay from other unconsolidated sediments because of its strong IP response (Breede and Kemna, 2012, Gazoty et al., 2012b). The metallic content of solid waste generates high chargeability, which makes demarcation of the waste boundaries at landfill sites using IP surveys plausible (Ustra et al., 2012). However, the chargeability status of the disseminated contaminant plume requires a comprehensive evaluation. The correct assessment of

the IP response produced by diffused leachate plumes is critical to the adequate characterization of contaminated sites. However, this topic is still under discussion. Some authors delineate dispersed waste free plumes as high chargeability zones (Abu-Zeid et al., 2004, Martinho and Almeida, 2006, Ustra et al., 2012), whereas Gallas et al. (2011) postulated that disseminated plumes exhibit low chargeability in host sediments, despite the high ionic content.

Dahlin (2010) overlaid the resistivity and chargeability models, and this integration considered the mixture of leachate and waste as a region of high chargeability combined with low resistivity. The resistivity models demarcated the leachate zones while chargeability models delineated the waste areas. These results suggest that the leachate plume is either susceptible to a resistivity evaluation rather than an IP assessment or the contaminant plume areas indicated insignificant IP responses. Their findings, which were results of the pre-excavation survey at a landfill site in Johannesburg, South Africa, also confirmed that solid waste and uncontaminated saturated soil have similar resistivity responses, and, therefore, cannot be differentiated using resistivity models. Nevertheless, the chargeability evaluation indicated the waste had a high IP response, and the saturated soil (not clay) had weak IP signals. The diversity in resistivity and chargeability values of various subsurface sections at a landfill site requires a simplified template for the interpretation of these regions.

Additionally, with the sprawl of new settlement over landfill sites, there is a vital need to develop and improve upon the municipal solid waste disposal processes in the urban and rural suburbs. The unregulated landfills and dumpsites have to be upgraded to sanitary status to safeguard the environment from the ground and surface

water contamination. In an update of uncontrolled landfills to sanitary level, the appraisal for the quantity of leachate is essential for the design of leachate collection channels and treatment plants (Kortegast et al., 2007). Precise evaluation of the extent of transportation of leachate establishing its flow direction and the estimate of its quantity are of paramount importance for a remediation. The appraisal on waste and leachate zones can serve as a component of hazard assessment, and this also assists in the placement of monitoring wells (Woldt et al., 1998).

In a bioreactor landfill set up, the sites operate on uniform moisture distribution in waste sections to aid the biodegradation (Barlaz et al., 2010). The customary methods of investigation of moisture content at these landfills are sampling through drilling, moisture sensors, and probe measurements (Imhoff et al., 2007). Apart from been invasive, weak contact is exhibited between the waste and the sensors. The responses from these approaches are localized, and they do not give a general view of the landfill sites (Shihada, 2011). These disposal sites require both overall and sectional moisture evaluation to improve upon the landfill performance, which could be determined effectively with surface geoelectrical imaging.

The adopted methodologies for estimating the amount of leachate for improved landfill practice such as WBM (Water Balance Method) and HELP (Hydrologic Evaluation of Landfill Performance) are based on water balance evaluation (Donevska et al., 2010, Zoqi and Ghavidel, 2011, São Mateus et al., 2012, Aziz et al., 2012, Alslaibi et al., 2013, Nas and Nas, 2014). These models predict the amount of leachate migrating from one layer to another on a landfill site using several storage centres. However, these approaches do not provide universal solutions to the current difficulties encountered in developing countries. The models use parameters that are

difficult to obtain, such as field capacity and wilting point (Aina et al., 2012). Moreover, the water balance procedure is a function of the change in moisture content within the waste, and this variation in landfills depends on the precipitation, evaporation rates, and field capacity.

The prediction models have limitations due to the uncertainties related to rainfall data and other required properties of landfill compositions (Kortegast et al., 2007). With the anticipated changes in the climate, there is the growing need to develop hydrogeological models for predicting water flows at the landfill sites (Gazoty et al., 2012b). Alternative processes for estimating the spatial spread and in situ quantity of leachate are essential for an upgrade or remediation of unregulated landfills and dumpsites. Geophysical methods are equipped tools to delineate and estimate the magnitude of aquifers and subsurface contamination. Woldt et al. (1998) integrated electromagnetic method and a geostatistical tool to screen an unregulated landfill, mapping the contaminant leachate and obtaining an approximation of the spatial extent of the waste and leachate.

1.3 Research objectives

This study integrated resistivity and IP methods at three landfill sites for subsurface characterization and contaminant plume mapping. The projected tasks are to:

(i) assess the prospects of IP data acquisition using the standard resistivity meter and conventional steel electrodes.

(ii) evaluate the chargeability status of the diffused contaminant plume with the aid of the geoelectrical and geochemical probes.

(iii) develop a simplified interpretation template for the integrated analysis of 2D resistivity and IP inverse models generated at the landfill sites.

(iv) appraise the performance of the leachate ponding, establish the flow direction of the pollutants, and g**au**ge the extent of percolation into aquifer receptors due to discharge from the aeration ponds and leakages from the landfill.

(v) explore an alternative approach to water balance methods for estimating the quantity of leachate at the downstream of a landfill site using 3D geoelectrical imaging.

1.4 Scope and limitations of the study

The three waste disposal sites selected for this study are within unconsolidated sediments. However, the procedure for the subsurface landfill classification and the leachate assessment could be implemented in a different geological setting. The site characterization demarcates the extent of waste deposits and contaminant plume while the identification of the quality of the waste that would determine the prospects of mining at a landfill site is not within the scope of the research. The subsurface characterization is limited to 2D resistivity/IP imaging profile while the leachate mapping and quantification displays a 3D estimation. The estimate of the leachate plumes in the study was conducted using a controlled discharge. However, the procedure of quantification can be applied to leachate plume in a regular preferential pathway.

The layout restriction at all the sites limits the depth of probes. The constraint is more pronounced in the landfills selected for delineation because some parts of the landfill have significant aquifer and waste depths. It is important to note that while the

subsurface characterization profiles show continuity in the interpretation of the sections, the profile intervals of 50 m could miss some traces of waste and leachate.

1.5 Thesis outline

The thesis consists of five chapters, summarized as follows:

Chapter 1 presents an introduction to the thesis that includes the background of the study, problem statements, scope and limitations, and organization of the thesis.

Chapter 2 has the literature review on a general appraisal of geophysical surveys and previous studies on municipal solid waste landfill sites. The section also presents the fundamental principles of electrical resistivity and IP techniques, with discussions on instrumentation, data acquisition, and data inversion procedures.

Chapter 3 describes the location, climate, and geology of the sites chosen for this research. The procedures involved in data acquisition, data processing, and interpretation are discussed in this chapter.

Chapter 4 presents experimental results and the discussions of the results. The outcomes of activities described in Chapter 3 are analyzed here. Additionally, statistical analyses were conducted on geophysical and physiochemical data.

Chapter 5 summarizes the significant conclusions from the research, stating the contributions from this work, and providing recommendations for further investigations.

CHAPTER 2

LITERATURE REVIEW

2.1 Introduction

The objective of this research centred on the characterization of landfill sites and the contaminant plume imaging. Consequently, the discussions for the review focused mainly on the two geoelectrical techniques adopted for these investigations. However, while the resistivity methods have exhausted literature given several case histories available in landfill applications, the utilization of IP techniques remain modest at solid waste disposal sites. The section attempts to present the justification for the integration of the two methods and the need for further effort in exploring the potential of the IP approach while overcoming the fundamental challenges inherent in its data acquisition and interpretation.

2.2 Review of geophysical techniques

Geophysical methods provide a complementary approach to the traditional drilling and sampling used in the earth sciences and engineering applications. These technologies, which are non-invasive and cost-effective, can explore large subsurface volumes by supplying continuous data. The geophysical application identifies targets for intrusive investigations and fills the gaps between several sampling points. The choice of exploration methods at a site is based on the physical property of the desired target. The target could be mapped where there is a local variation in a measured parameter about some background value.

More often than not, two or more geophysical techniques are combined to improve the quality of interpretation. Supplementary approaches could resolve the ambiguity in the analysis of a method. While some methods are best suited for reconnaissance surveys, others may be robust to a detailed coverage. Kearey et al. (2002) present a clear classification of geophysical methods with the corresponding measured data and the operative physical property of the subsurface (Table 2.1). Additionally, Table 2.2 shows the main fields of geophysical methods indicating the most appropriate techniques for the various applications.

Table 2.1 Classification of geophysical methods [after Kearey et al. (2002)]

Method	**Measured Parameter**	**Operative Physical Property**
Seismic	Travel times of seismic waves	Density and Elastic moduli
Gravity	Spatial variations in the strength of the gravitational field of the Earth	Density
Magnetic	Spatial variations in the strength of the geomagnetic field	Magnetic susceptibility and remanence
Electrical resistivity	Earth resistance	Electrical conductivity
Induced polarization	Polarization voltages or frequency-dependent ground resistance	Electrical capacitance
Self-potential	Electric potentials	Electrical conductivity
Electromagnetic	Response to electromagnetic radiation	Electrical conductivity and inductance
Radar	Travel times of reflected radar pulses	Dielectric constant

Table 2.2 Applications of geophysical methods [after Kearey et al. (2002)]

Application	Appropriate techniques
Exploration for fossil fuels	S, G, M, (EM)
Exploration for metallic minerals	M, EM, E, SP, IP, R
Exploration for bulk minerals (sand and gravel)	S, (E), (G)
Exploration for underground water	E, S, (G). (GPR)
Engineering site investigations	E, S, GPR, (G), (M)
Archaeology investigations	GPR, E, EM, (M), (S)

* G, gravity; M, magnetic; E, electrical resistivity; SP, self-potential; IP, induced polarization; S, seismic; EM, electromagnetic; GPR, ground-penetrating radar; R, radiometric. Subsidiary methods are in brackets.

2.3 Previous geophysical studies on landfills

In a reconnaissance survey for either restoration or remediation of landfill sites, geophysical methods could determine the edge and depth of the deposited solid waste. The critical environmental application involves a delineation of impacted groundwater and the contaminant pathway at solid waste dumpsites added to a continuous leak detection monitoring. Time domain and frequency domain electromagnetic (EM) methods are employed for delineating waste site boundaries and mapping shallow plume. Moreover, the results from this probe could be used to identify where to install monitoring wells.

The magnetic methods are valuable to locate and delineate buried metal debris such as drums and tanks. Gravity appraisal is a ready tool to map the boundaries of deposited waste given the density contrast between the landfill and host sediments or host rocks. Induced polarization, Self-potential (SP), electrical resistivity and Ground Penetrating Radar (GPR) are applied to map contaminant plumes and locate buried waste. Seismic methods could discern the geometry and depth of landfills.

Although gravity method is rarely used at landfill sites, Silva et al. (2009) mapped buried landfill bottom topography with gravity data. The gravity inversion estimates the landfill's depth at discrete points with a decrease of the density contrast with depth. In situ monitoring of moisture circulation and variations in mechanical properties of municipal solid waste (MSW) is needed to optimize the safe and efficient operation of landfills. Carpenter et al. (2013) employed seismic surveys to apprehend the changes in shear modulus and Poisson's ratio of solid waste to infer the extent of degradation and offer dynamic properties needed for seismic stability evaluation. To obtain the desired result, a series of seismic surveys were performed at a landfill site in the USA to image seismic velocity structure and the Poisson's ratio of a recirculation cell and compared with an adjacent newer landfill cell in the absence of leachate recirculation. Seismic data were acquired using fan shot direct P-wave surveys and S-wave surveys, conventional P-wave refraction, and the multichannel analysis of surface waves (MASW) technique.

Prezzi et al. (2005) show the results of a ground magnetic survey carried out to study solid waste landfills. The total magnetic field was assessed along six profiles on a landfill site. The profiles were modelled in 2.5 D, and along with them, an estimate of depth to the sources was determined by Euler's deconvolution procedure. The first and the second derivatives of the residual magnetic field were calculated, to sharpen the anomalies. The interpretation shows that the characteristics of the modelled bodies and the magnitudes of the detected anomalies do not confirm the presence of drums in the sanitary infill.

De Carlo et al. (2013) present geophysical results of a study observed on a dismissed landfill, near to the city of Corigliano d'Otranto, in the Apulia region

(Southern Italy). The landfill is located in an abandoned quarry; that was subsequently reutilized after thirty years as a site for solid waste disposal. The waste was about 20 m thick, and the landfill bottom was expected to be lined with an HDPE (high-density polyethylene) material. During the digging operations to build a nearby new landfill, leachate was found, which triggers an in-depth investigation. The major goal was to verify whether the leachate is leaked through by the HDPE liner. Both surface electrical resistivity imaging, and mise-à-la-masse (MALM) surveys were conducted despite the challenges of the rugged terrain of the deserted quarry complex. A conductive body, probably associated with leachate, was found as deep as 40 m below the current landfill surface at a depth much greater than the expected 20 m thickness of waste. Because of the logistical difficulties that limit the geometry of acquisition, synthetic forward modelling was used to confirm or dismiss interpretational hypotheses emerging from the electrical resistivity and MALM results. This integration between measurements and modelling helped narrow the alternative interpretations and strengthened the confidence in results.

Quantifying thin-layer parameters accurately by supplying a targeted reflection waveform inversion process to ground-penetrating radar (GPR) reflection data may offer a useful tool for near-surface study and especially for contaminated site probe expecting the presence of nonaqueous phase liquid (NAPL) contaminants. Babcock and Bradford (2015) implemented a targeted reflection waveform inversion algorithm to quantify thin-layer permittivity, thickness, and conductivity for NAPL thin and ultra-thin layers using GPR reflection. The inversion used a nonlinear grid search with a Monte Carlo scheme to set the starting values to find the universal minimum. By taking a targeted procedure using a time window around the peak amplitude of the

reflection event of interest, the algorithm reduced the complexity in the inverse problem. The inversion was tested on four field data sets and three different synthetic data sets. In all testing, the inversion resolved for NAPL-layer properties within 15% of the measured values. The algorithm provides a tool for site managers to prioritize remediation efforts based on quantitative assessments of contaminant quantity and location using GPR.

A combination of two or more geophysical methods is adopted for a full characterization of a landfill site to minimize the interpretation ambiguity in surveys. The diverse makeup of dumpsite's subsurface desires cocktail of geophysical tools to map the in-situ multi-character constituents. Martínez and Mendoza (2011) deployed the use of electrical resistivity, EM, Magnetics, and seismic refraction technique at two landfill sites in Denmark. In the first case, electrical resistivity tomography was applied to assess the sealing condition in new cells within a landfill complex. The survey was to ensure that the in situ soil within 2-3 m has adequate and uniformly distributed clay content. At the other landfill, detailed preliminary studies were carried out using EM and Magnetic methods for mapping and locating three UXO (Unexploded Ordnance) devices. After the clearance of the devices, geotechnical drillings characterized the soil to suggest points for groundwater monitoring and to evaluate the limestone for seismic refraction correlation. The seismic appraisal provided information that recommends the maximum vertical digging depth for the planned expansion of the site for polluted soil. The variation in thickness of the clay till above the limestone presented possibilities of higher storage volumes if deep excavations were allowed in areas where the limestone surface was deeply buried. The depth of the excavation should be designed to prevent hydraulic uplift of the clay turnover during excavation and filling.

Electrical resistivity, self-potential (SP), and very low frequency electromagnetic (VLF-EM) surveys were carried out at an open waste disposal site in Çanakkale, Turkey. The objective of the investigation is to detect and map the spread of groundwater contamination and locate possible pathway of leachate plumes (Kaya et al., 2007). The results of the study showed a low resistivity zone (< 5 Ωm) as the leachate plume, and this was confirmed with the VLF-EM and SP mappings. High negative values exhibited from VLF-EM and SP data determined the vertical contact between the contaminated and uncontaminated zones.

Dawson et al. (2002) combine geophysical and borehole techniques to investigate the hydrogeology controlling the transport of leachate from Winthrop Landfill, Maine, in the USA to the nearby Annabessacook Lake. A combination of borehole EM, 2D resistivity, seismic reflection, and magnetic surveys was conducted to gauge the preferential flow of the contaminant plume. The study identified shoreline seep signatures, hidden seeps in the lake, and depth to the bedrock within the lake. The interpretation of the data delineates an electrical conductive anomaly consistent with the contaminant plume moving from the landfill boundary southward through the overburden to the shores of the lake. The results of the study also indicated the discrete, shallow, and conductive anomalies at the south-eastern edge of the landfill and near to the lakeshore. The magnetic data confirmed the presence of iron-rich plume discharging into the lake. The seismic survey mapped the sediment and its grain size distribution, where the sediment-infilled bedrock may act as a conduit for contaminant migration.

A joint application of electrical resistivity tomography, VLF-EM, EM conductivity, seismic refraction, ambient noise seismic, and chemical analysis was

employed for the characterization and management of a landfill site in Crete Island, Greece (Soupios et al., 2007). Both electrical resistivity imaging and EM ground conductivity techniques were conducted to determine the spatial distribution of leachate plume. Also, the resistivity profile identified the depth and thickness of the buried waste and the variation of moisture content to ensure decomposition of organic waste. The seismic ambient noise analysis established the slope site performance and emphasizing that the permanent deformation of the study area be due to the earthquake loading. However, the VLF-EM results were without required precision because of the steep topography, difficulty in finding appropriate VLF transmitters and high interference from surface metallic surface objects. In contrary, the seismic refraction data correlated with the geoelectrical profile, and it was used as the confirmation probe.

Table 2.3 presents a summary of applications of the individual geophysical method in landfill investigation. It is pertinent to note that while additional tools reduce the ambiguity in the interpretation of the desired targets, the cost of surveys should be a factor of interest to the geophysicist. A compromise between the number of techniques, logistics, and cost should be the basis for the choice of appropriate geophysical tools for an investigation. Reynolds (1991) presents a flow chart to illustrate decision-making process leading to the selection of geophysical methods and utility software for a prospective survey (Fig. 2.1).

Table 2.3 Summary of application of geophysical surveys at landfill sites

Geophysical Technique	**Potential application to landfill investigation**
EM	Edge of waste delineation Shallow plume mapping Distinguish wet and dry areas Delineate metallic drums
SP	Map contaminant plume Locate buried waste Identify contaminant plume leakages
IP	Map contaminant plume Locate buried waste and delineate its boundaries Differentiate waste mass from background geology
Resistivity	Map contaminant plume Locate buried waste Characterize composition of landfill material Examine integrity of cap and liner material
Magnetic	Delineate metallic debris
Gravity	Delineate waste boundaries Determine landfill depth
GPR	Map contaminant plume Locate buried waste
Seismic	Delineate waste boundaries Determine landfill depth

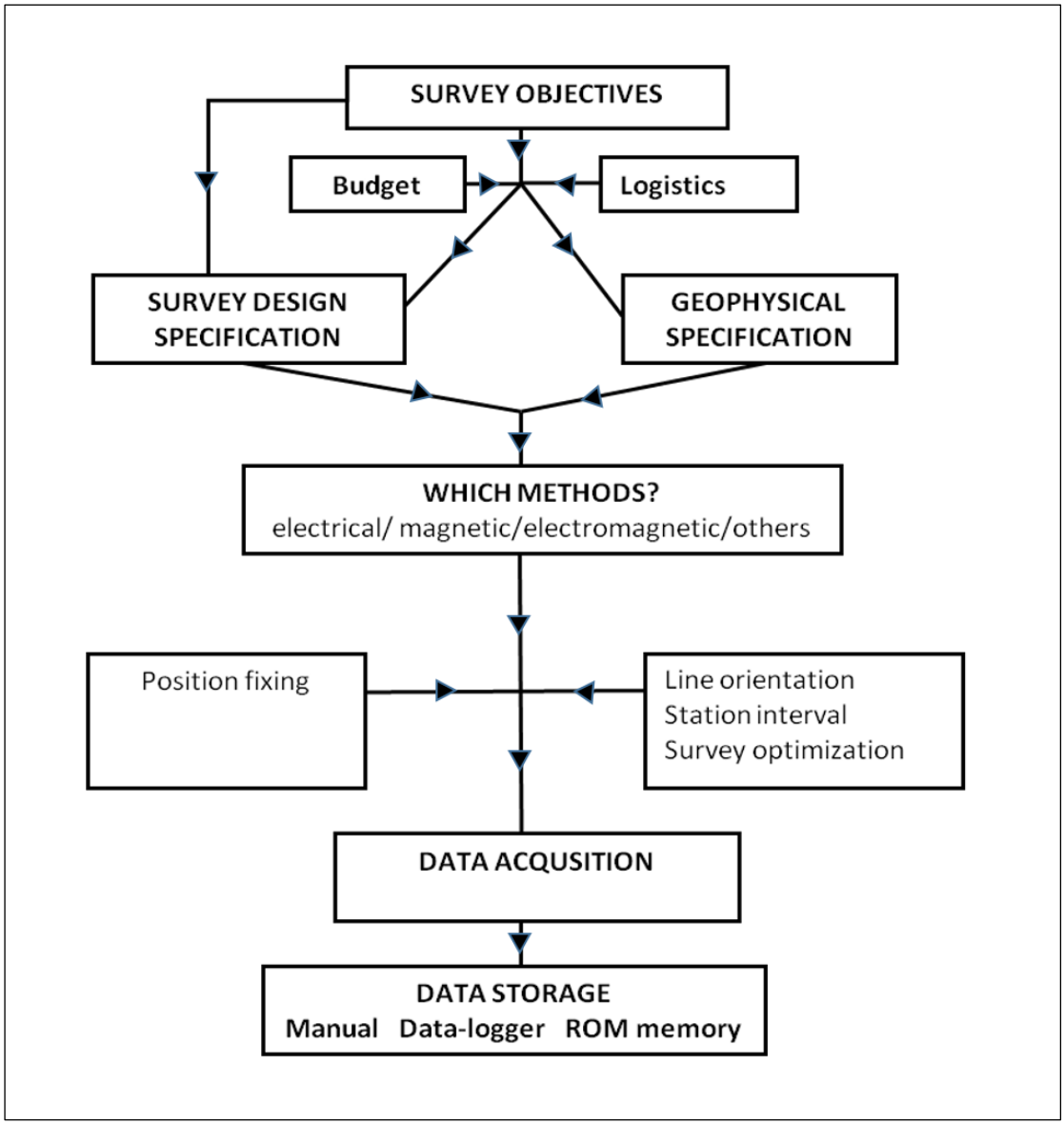

Figure 2.1 Decision-making process leading to the selection of geophysical methods and utility software for an investigation [adapted from (Reynolds, 1991)]

2.4 Joint resistivity/Induced Polarization (IP) surveys at landfill sites

IP survey has advantages over the EM and Magnetic methods that are traditional methods for characterization of waste disposal areas. IP and electrical resistivity data can provide more vertical information than that of EM and unlike magnetics, the IP methods can delineate non-metallic waste. Vertical data is vital as it is a recognized factor in determining the cost of remediation to estimate the quantity of waste. Also, this vertical column is usually in the plan for future use of the landfill site (Carlson et al., 2001).

IP survey is widely used in exploration for ore bodies, mainly for disseminated sulphides. The IP effect due to sulphide mineralization (the electrode polarization effect with about 100 to 200 mV/V range) is much higher than that due to clay minerals (membrane polarization) in siltstones and sandstone. The chargeability of clays is within the 10 to 50 mV/V range that is much smaller than that due to conductive minerals (Šumi, 1965). However, negative IP effects have been reported for certain types of clays (Brandes and Acworth, 2003). Another application of IP in environmental surveys is the detection of decomposing organic matter (Weller et al., 2000).

The high IP effect of disseminated metallic sulphides makes IP surveys an attractive tool for exploration of such minerals. The contrast in resistivity for such deposits is frequently low due to its disseminated nature that makes detection by normal resistivity, and EM surveys difficult (Loke, 2015). The use of IP in geotechnical and engineering applications has been limited while been used principally for groundwater exploration. However, in recent years, there has been an increasing

amount of literature on the integration of resistivity and IP techniques for characterization and contaminant plume mapping at landfill sites.

As stated earlier in Chapter 1, IP techniques complement electrical resistivity methods in the characterization of the landfill's subsurface. The application of IP procedure works in situations where ground-truth data are not available for calibration in the field. The process detects "where the waste is", and the use of both the IP and resistivity could estimate "what the waste is" (Carlson et al., 2001). Martinho and Almeida (2006) integrated electrical resistivity and IP measurements to define a valid spatial contamination model in the vicinity of two municipal landfills in Portugal. In both landfills, negative IP values were detected associating with the positive IP values; this could be explained by the 2D and 3D geometric effects generated by the presence of the contaminant plumes.

The combination of IP and electrical resistivity surveys was also used to map waste deposits and demarcate important geological units. These geological units appear to control the hydrology of a decommissioned landfill site in Hørløkke, Denmark (Gazoty et al., 2012b). The results display a silt/clay lens at a depth that correlates the contaminant plume flow direction as it spreads out from the landfill. The outcome also reflects a shallow sandy layer rich in clay that has an effective influence on the hydrology of the site. Several other workers combined resistivity and IP surveys in mapping contaminant plume and delineation of waste disposal sites (Rosqvist et al., 2003, Johansson et al., 2007, Leroux et al., 2007, Mondal et al., 2010, Ustra et al., 2012).

2.5 Landfills in Malaysia

By 2012, there were 296 municipal solid waste disposal sites in Malaysia under the management of local authorities (Table 2.4). Most of these places are open, unregulated dumpsites, and the capacity has been overloaded. Figure 2.2 shows an active and closed open dump sites in Kuala Terengganu, Terengganu and Parit Buntar, Perak respectively. Fauziah and Agamuthu (2012) classified landfills in Malaysia based on available facilities (Table 2.5) and listed 12 to be of sanitary status (Table 2.6). One of the sanitary landfills is in Bukit Tagar, in the state of Selangor. The landfill has a containment facility and leachate recirculation system. The procedures include SBR (Sequencing Batch Reactors) at aeration points and subsequent use of Reed beds. Furthermore, a green high-density polyethylene liner is placed on soil covering the waste to optimize methane gas extraction for a power generating plant (Fig 2.3).

Table 2.4 Existing landfills sites in Malaysia [after JPSPN, Malaysia (2012)]

State	Operating landfills	Closed landfills	Total in state
Johor	14	23	37
Kedah	8	7	15
Kelantan	13	6	19
Melaka	2	5	7
Negeri Sembilan	7	11	18
Pahang	16	16	32
Perak	17	12	29
Perlis	1	1	2
Pulau Pinang	2	1	3
Sabah	19	2	21
Sarawak	49	14	63
Selangor	8	14	22
Terengganu	8	12	20
WP Kuala Lumpur	0	7	7
WP Lubuan	1	0	1
Total	165	131	296

(a) Active site

(b) Closed site

Figure 2.2 Open dumpsites in Malaysia (a) Active site in Kuala Terengganu (b) Closed site at Parit Buntar, Perak